

Insulin-stimulated glucose uptake in skeletal muscle, adipose tissue and liver: a positron emission tomography study

Miikka-Juhani Honka¹, Aino Latva-Rasku¹, Marco Bucci², Kirsi A Virtanen^{1,3}, Jarna C Hannukainen¹, Kari K Kalliokoski¹ and Pirjo Nuutila^{1,4}

Turku PET Centre, ¹University of Turku, Turku, Finland, ²Åbo Akademi University, Turku, Finland, ³Institute of Public Health and Clinical Nutrition, University of Eastern Finland, Kuopio, Finland, and ⁴Department of Endocrinology, Turku University Hospital, Turku, Finland

Correspondence should be addressed to P Nuutila
Email
pirjo.nuutila@utu.fi

Abstract

Objective: Insulin resistance is reflected by the rates of reduced glucose uptake (GU) into the key insulin-sensitive tissues, skeletal muscle, liver and adipose tissue. It is unclear whether insulin resistance occurs simultaneously in all these tissues or whether insulin resistance is tissue specific.

Design and methods: We measured GU in skeletal muscle, adipose tissue and liver and endogenous glucose production (EGP), in a single session using ¹⁸F-fluorodeoxyglucose with positron emission tomography (PET) and euglycemic–hyperinsulinemic clamp. The study population consisted of 326 subjects without diabetes from the CMgene study cohort.

Results: Skeletal muscle GU less than 33 $\mu\text{mol}/\text{kg}$ tissue/min and subcutaneous adipose tissue GU less than 11.5 $\mu\text{mol}/\text{kg}$ tissue/min characterized insulin-resistant individuals. Men had considerably worse insulin suppression of EGP compared to women. By using principal component analysis (PCA), BMI inversely and skeletal muscle, adipose tissue and liver GU positively loaded on same principal component explaining one-third of the variation in these measures. The results were largely similar when liver GU was replaced by EGP in PCA. Liver GU and EGP were positively associated with aging.

Conclusions: We have provided threshold values, which can be used to identify tissue-specific insulin resistance. In addition, we found that insulin resistance measured by GU was only partially similar across all insulin-sensitive tissues studied, skeletal muscle, adipose tissue and liver and was affected by obesity, aging and gender.

European Journal of
Endocrinology
(2018) 178, 523–531

Introduction

Insulin resistance is a major feature in the development and pathophysiology of type 2 diabetes. In healthy individuals, skeletal muscle takes the major part of glucose uptake (GU) during hyperinsulinemia (about 75–80%), whereas the proportion of GU into adipose tissue and liver is substantially smaller (1). Individuals with normal weight and normal glucose tolerance are highly sensitive to insulin in skeletal muscle, adipose tissue and liver (2,

3, 4), whereas obese individuals and individuals with type 2 diabetes are insulin resistant (4, 5, 6). Decreased muscle GU, increased endogenous hepatic glucose production (EGP) and impaired insulin secretion contribute to hyperglycemia and type 2 diabetes (1).

Activation of the phosphoinositol 3-kinase/AKT2 pathway results in translocation of insulin-sensitive glucose transporter GLUT4 (SLC2A4) to the plasma

membrane and in an increase of glucose transport into muscle and adipose tissue (7, 8). In the liver, activated AKT inhibits the rate-controlling enzymes of gluconeogenesis resulting in the suppression of EGP and promotes glycogen synthesis (9, 10). Additionally, increased lipolysis from white adipose tissue promotes hepatic insulin resistance by increasing hepatic gluconeogenesis via an increased free fatty acid (FFA) flux into the liver (11). Glycogen is the main repository for GU in the liver (12). Additionally, FFAs, inflammatory cytokines and organokines can affect insulin sensitivity in various tissues (13, 14, 15).

Insulin sensitivity in humans has been previously addressed by evaluating whole body GU, EGP or suppression of lipolysis (16, 17, 18, 19, 20). The use of positron emission tomography (PET) with a positron-emitting glucose analog, ^{18}F -fluorodeoxyglucose (^{18}F FDG), allows the direct measurement of the rates of GU in multiple insulin-sensitive tissues. Combining this method with the measurements of whole body insulin sensitivity, the euglycemic-hyperinsulinemic clamp (21), allows us to directly assess tissue-specific GU or insulin sensitivity. Even though muscle GU is responsible for most of the whole body GU during euglycemic-hyperinsulinemic clamp, contribution of liver is higher after meal when liver takes up approximately one-third of an ingested glucose load and EGP is suppressed (12). Furthermore, contribution of adipose tissue on whole body GU is larger when fat mass is high (22, 23). Therefore, it is important to understand whether insulin resistance to GU and EGP suppression occur simultaneously in all these tissues or whether insulin resistance is tissue specific. To address this question, we collected a large cohort of non-diabetic individuals whose skeletal muscle, liver and adipose tissue insulin sensitivity have been measured using PET, ^{18}F -FDG and the euglycemic-hyperinsulinemic clamp.

Subjects and methods

Subjects

The subjects were 326 volunteers who had previously participated in PET studies at the Turku PET Centre (Turku, Finland) and who did not have diabetes according to the American Diabetes Association criteria (24) (Table 1). Women were older than men ($P < 0.001$) but no difference was observed in body mass index (BMI). All subjects gave a written informed consent. The study protocol was approved by the Ethics Committee of the Hospital District of South-West Finland and the study has been registered to ClinicalTrials.gov (NCT03310502).

Study design and methods

The PET studies were performed after an overnight fast. The subjects were instructed to avoid consumption of alcohol and caffeine for 12 h, and strenuous physical activity 24 h before the study. The subjects were in a supine position during the euglycemic-hyperinsulinemic clamp and PET scanning. A cannula was inserted in an antecubital vein for the infusion of glucose and insulin and the injection of ^{18}F FDG, and another cannula was inserted in the opposite upper extremity radial artery or antecubital vein that was warmed with a heating pillow to arterialize venous blood for blood sampling. Plasma glucose was maintained at euglycemia (~ 5 mmol/L) by a primed (first 4 min at 120 mU/body surface area m^2/min and then 3 min at 80 mU/body surface area m^2/min) and then continuous insulin infusion at 40 mU/body surface area m^2/min and 20% glucose infusion based on plasma glucose measurements taken every 5–10 min (21). The rates of whole body GU (M value) were calculated from steady state and reported as the average of three 20-min intervals, starting after reaching euglycemia (median

Table 1 Characteristics of the study participants. Data presented as mean \pm s.d.

	Men	Women	All	<i>P</i> (men vs women)
Number of participants	216	110	326	
Age (years)	40.2 \pm 15.3	53.4 \pm 16.8	44.6 \pm 17.0	<0.001
Body mass index (kg/m^2)	26.8 \pm 5.1	28.7 \pm 7.4	27.4 \pm 6.0	0.170
Fasting plasma glucose (mmol/L)	5.5 \pm 0.5	5.6 \pm 0.6	5.6 \pm 0.5	0.907
Fasting serum insulin ($\mu\text{U}/\text{mL}$)	8.8 \pm 6.2	8.9 \pm 6.5	8.8 \pm 6.3	0.815
Whole body GU ($\mu\text{mol}/\text{kg}$ body weight/min)	28.7 \pm 15.4	26.0 \pm 13.0	27.8 \pm 14.7	0.228
Femoral skeletal muscle GU ($\mu\text{mol}/\text{tissue}$ kg/min)	42.9 \pm 27.0	46.6 \pm 29.7	44.1 \pm 27.9	0.397
Liver GU ($\mu\text{mol}/\text{tissue}$ kg/min)	21.7 \pm 8.2	23.2 \pm 10.2	22.4 \pm 9.2	0.380
Subcutaneous adipose tissue GU ($\mu\text{mol}/\text{tissue}$ kg/min)	10.9 \pm 6.7	12.5 \pm 7.0	11.6 \pm 6.8	0.054
Intraperitoneal adipose tissue GU ($\mu\text{mol}/\text{tissue}$ kg/min)	18.0 \pm 10.2	24.9 \pm 12.4	21.3 \pm 11.8	<0.001
Endogenous glucose production ($\mu\text{mol}/\text{kg}$ body weight/min)	7.0 \pm 6.3	3.1 \pm 4.6	5.1 \pm 5.9	<0.001

GU, glucose uptake.

60 min from the start of insulin infusion). [¹⁸F]FDG was injected at average 80 (interquartile range 60; 101) min from the start of insulin infusion, and dynamic scans were performed to get images of abdomen and femoral regions as previously described (25, 26). The timing when each region was scanned varied according to the original PET research protocol. Plasma radioactivity was measured from arterial or arterialized blood samples.

Measurements of skeletal muscle, liver and adipose tissue glucose uptake

[¹⁸F]FDG was synthesized using a modified method of Hamacher *et al.* (27). PET-scanners ECAT 931/08 (Siemens Molecular Imaging, Inc., Knoxville, TN, USA), GE Advance, PET/CT Discovery VCT and PET/CT Discovery 690 (General Electric Medical Systems, Milwaukee, WI, USA) tomographs were used. The scanners were cross-calibrated against the same VDC-404 Dose calibrator (COMECER Netherlands, Joure, the Netherlands) to ensure the consistency of the results. All data obtained were corrected for dead time, decay and measured photon attenuation. The Bayesian iterative reconstruction algorithm, using median root prior with iterations and a Bayesian coefficient of 0.3, was used for image processing when possible (28). Tissue-specific GUs were measured by drawing the regions of interest (ROI) to quadriceps femoris, right lobe of the liver and abdominal subcutaneous and intraperitoneal adipose tissue. MRI or CT images were used as references for outlining the regions.

The rates of liver, skeletal muscle and adipose tissue GU were calculated by graphically analyzing plasma and tissue time–activity curves to quantify the fractional phosphorylation rate (K_i) for [¹⁸F]FDG (29, 30). The rates of GU were calculated by multiplying K_i by the plasma glucose concentration and dividing by the tissue density and a lumped constant. A lumped constant corrects for the differences in transportation and phosphorylation of [¹⁸F]FDG and glucose. A lumped constant value of 1.0 for liver, 1.2 for skeletal muscle and 1.14 for adipose tissue were used (25, 26, 31).

Measurement of endogenous glucose production

EGP during the clamp study was measured using a previously validated method (32). In brief, ¹⁸F-FDG clearance adjusted with ¹⁸F-FDG lost to urine was used to determine glucose rate of disappearance. EGP was calculated by subtracting glucose infusion rate from glucose rate of disappearance. Possible changes in glucose

level over the study were accounted by adding a space correction (21) to glucose infusion rate.

Biochemical analyses

Plasma glucose during the euglycemic–hyperinsulinemic clamp was determined in duplicate by the glucose oxidase method (Analox GM7 or GM9, Analox Instruments, London, UK). Serum insulin concentration, determined every 30 min during the clamp, was measured by a double antibody RIA (Phadeseph Insulin RIA kit, Pharmacia & Upjohn, Uppsala, Sweden) or automatized electrochemiluminescence immunoassay (Cobas 8000, Roche Diagnostics GmbH), and serum FFA concentration, determined every 60 min during the clamp was measured using an enzymatic assay (ACS-ACOD, Wako Chemicals GmbH, Neuss, Germany).

Correlation testing and group comparisons

Statistical testing was done using IBM SPSS Statistics for Windows (version 23; IBM). Pearson correlation test was used to assess linear associations of the rates of tissue GU. GU values were log-transformed to achieve normal distribution. *T*-test or Mann–Whitney *U*-test was used to compare men and women or insulin-resistant and insulin-sensitive groups. The notched boxplots were created using ggplot2 package (33) of R statistical computing environment (version 3.4.1) (34).

Principal component analysis

Principal component analysis (PCA) and correlation testing were used to assess the association between the rates of tissue GU. PCA is a dimension reduction technique, which aims to combine several correlated variables to smaller number of components that explain most of the variation in the original variables thus allowing to find underlying patterns in the data (35). Eigenvalue 1.0 was used as a threshold value in PCA (36).

Receiver-operating characteristics curve analysis

We used receiver-operating characteristics (ROC) curve to find a cutoff value to divide our population to insulin-sensitive and -resistant subjects. Stern *et al.* (37) have previously provided a threshold for insulin resistance based on whole body GU per fat-free mass. Since we did not have body fat mass measurement required for this original threshold for all our subjects, we used ROC

analysis to find a corresponding value expressed per body weight. The found cutoff 21 $\mu\text{mol}/\text{kg}$ body weight/min had sensitivity 92% and specificity 99% with the original cutoff of 28 $\mu\text{mol}/\text{kg}$ fat-free mass/min. It presented the lowest 10% of normal-weight subjects ($\text{BMI} < 25 \text{ kg}/\text{m}^2$) and highest 16% of obese subjects ($\text{BMI} \geq 30 \text{ kg}/\text{m}^2$) in our study cohort. Based on this cutoff, ROC curve analysis was used to find optimal thresholds for skeletal muscle and adipose tissue GU and EGP. Area under ROC curve over 0.7 is considered acceptable for discrimination (38). Analysis was performed separately according to sex where there was difference between sexes in tissue GUs or EGP.

Results

Associations between glucose uptake rates and EGP in different sexes

In men and women, the M value correlated strongly and significantly with skeletal muscle GU ($r=0.910$ and 0.877) and subcutaneous GU ($r=0.360$ and 0.621 , correspondingly; $P=0.015$ between men and women) (Fig. 1), whereas the correlations of the M value with liver GU ($r=0.187$ and 0.287) were considerably weaker. The correlation of skeletal muscle GU with subcutaneous GU was statistically significant in both genders ($r=0.303$ in men and 0.520 in women), but correlation of skeletal muscle GU with liver GU was non-significant ($r=0.171$ and 0.189 , correspondingly) in both genders. BMI correlated inversely with GUs in all tissues examined (skeletal muscle $r=-0.583$, $P<0.001$; liver $r=-0.173$, $P=0.009$; subcutaneous adipose tissue $r=-0.364$, $P<0.001$).

EGP during the clamp was inversely and significantly correlated with the M value in women but only weakly in men ($r=-0.247$ and -0.464 in men and women, respectively, Fig. 2). EGP correlated inversely with skeletal muscle GU in men and women ($r=-0.247$ and -0.322 , correspondingly). Inverse correlation of EGP with subcutaneous adipose tissue and liver GU was observed in women ($r=-0.275$ and -0.233), but in men, there was a weak positive correlation of EGP with adipose tissue and liver GU ($r=0.267$ and 0.103 , respectively). When testing the correlation between EGP and intraperitoneal adipose tissue, there was no association in either men ($r=0.180$, $P=0.147$) or women ($r=-0.090$, $P=0.521$).

A possible mediator between the associations of tissue GUs is the concentration of FFAs during the clamp. Significant inverse correlations of tissue GUs and FFA

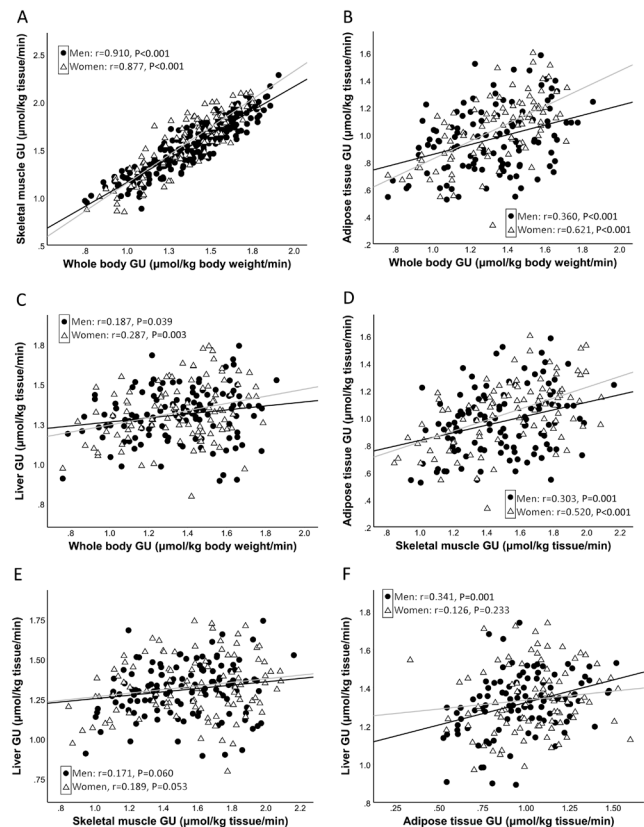


Figure 1

Correlation of whole body glucose uptake (GU) with skeletal muscle GU (A), subcutaneous adipose tissue GU (B) and liver GU (C); correlation of skeletal muscle GU with subcutaneous adipose tissue GU (D) and liver GU (E); and correlation of subcutaneous adipose tissue GU with liver GU (F). GU values are from log₁₀ transformed variables. Black regression line: men; gray regression line: women.

level during the clamp were observed in skeletal muscle ($r=-0.333$, $P<0.001$), adipose tissue ($r=-0.551$, $P<0.001$) and liver ($r=-0.214$, $P=0.005$). FFAs during the clamp were higher in men than in women (0.12 (interquartile range 0.08–0.17) vs 0.05 (0.03–0.08) mmol/L, $P<0.001$). Insulin and glucose levels during the clamp were 65 (57–82) mU/L and 5.1 (4.8–5.3) mmol/L.

Cutoff values for muscle and adipose glucose uptake rates

Based on ROC curve analyses, the optimal cutoff points for tissue-specific insulin sensitivity were calculated for men and women. Skeletal muscle GU of 33 $\mu\text{mol}/\text{kg}$ tissue/min separated insulin-sensitive and insulin-resistant subjects in ROC analysis (sensitivity 86% and specificity 89%)

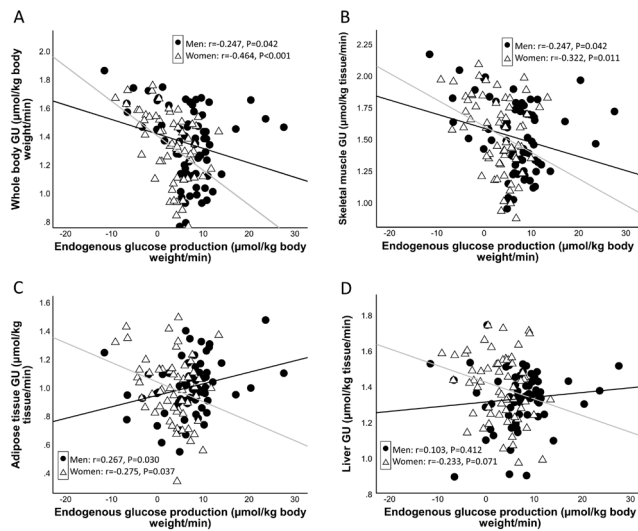


Figure 2

Correlation of endogenous glucose production with whole body glucose uptake (GU) (A), skeletal muscle GU (B), subcutaneous adipose tissue GU (C) and liver GU (D). GU values are from log₁₀ transformed variables. Black regression line: men; gray regression line: women.

(Fig. 3). The cutoff for skeletal muscle GU presented the lowest 22% in normal-weight subjects and the highest 21% obese individuals. Skeletal muscle and adipose tissue were clearly insulin resistant in subjects with whole body insulin resistance, while insulin-stimulated liver GU was only slightly lower compared to the insulin-sensitive group (Fig. 3). We found that 11.5 µmol/kg tissue/min separated insulin-resistant subjects most accurately in both men and women, though area under ROC curve was less than 0.7 in men. Similarly, 3 µmol/kg body weight/min was found as optimal cutoff for EGP in both sexes but area under ROC curve was less than 0.7 in men. Liver GU between high and low insulin sensitivity groups was different only when not separating the population by sex and a good cutoff could not be found. Insulin suppression of EGP was worse in the insulin-resistant group, though the difference was not significant among men. Men had worse suppression of EGP compared to women (Table 1).

Relationships between tissue insulin sensitivities, age, BMI and sex

Principal component analysis was used to study the relationships between tissue insulin sensitivities, age, BMI and sex. The results of PCA performed separately for men and women are shown in Table 2. The first principal component, PC1 (Model 1), including age,

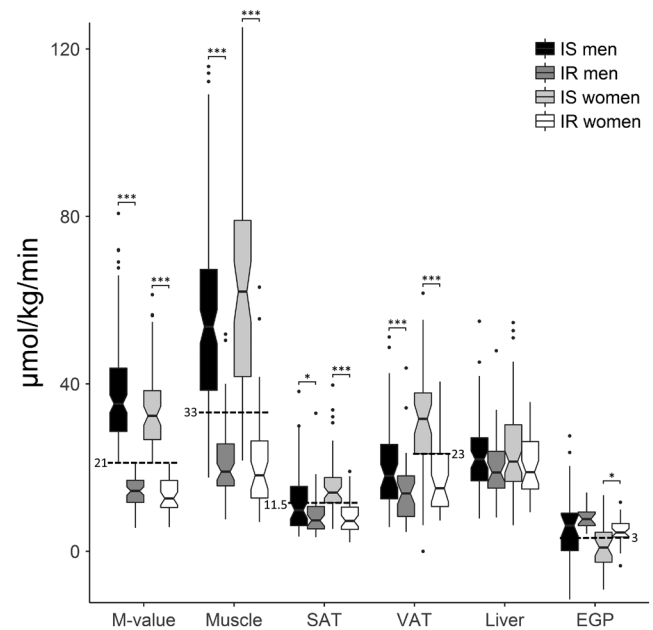


Figure 3

Whole body (*M* value), muscle, subcutaneous adipose tissue (SAT), intraperitoneal adipose tissue (VAT) and liver glucose uptake and endogenous glucose production (EGP) between insulin-sensitive (IS) and -resistant (IR) men and women. Dashed lines represent the optimal cutoff values between insulin-resistant and -sensitive individuals. The middle, bottom and top edges of the boxes represent median with 1st and 3rd quartiles, and notches are calculated as $1.58 \times$ interquartile range/square root (*n*) (95% confidence interval for the median). If notches do not overlap, there is evidence for a difference between medians. The error bars extend to the furthest case inside 1.5 interquartile range from the box and outliers are presented as dots. *** $P < 0.001$, * $P < 0.05$.

BMI and skeletal muscle and subcutaneous adipose tissue GU, explained 45% of the variation in men and 49% in women. Both skeletal muscle and adipose tissue GU had high positive and BMI negative loadings on PC1. PC2 was characterized by the effects of age in both genders. When combining men and women in PCA, the results remained largely unchanged. After adding liver GU in the model (Model 2), the variance explained was reduced to 38% in men and 39% in women attributable to the differences between the genders in liver GU (high loading only in men). The loading of liver GU on PC1 was substantially lower than those of skeletal muscle and adipose tissue in women suggesting a gender difference in the contribution of liver GU to the loadings on PC1. PC2 explained 27 and 32% of the variation in men and women, correspondingly, and was characterized by the

Table 2 Principal component analysis. Loadings in men and women indicate the contribution of each variable (GU, glucose uptake) to principal components (PC1, PC2, PC3).

GU ($\mu\text{mol/kg tissue/min}$)	Men		Women		All		
	PC1	PC2	PC1	PC2	PC1	PC2	PC3
Model 1							
Age (years)	-0.205	0.895	-0.006	0.952	0.095	0.693	-
Body mass index (kg/m^2)	-0.857	0.023	-0.724	-0.489	-0.829	0.108	-
Gender	-	-	-	-	-0.033	0.822	-
Skeletal muscle GU	0.833	-0.091	0.850	0.126	0.830	0.015	-
Subcutaneous adipose tissue GU	0.585	0.617	0.841	-0.206	0.703	0.240	-
Variance explained (%)	45	30	49	30	38	25	-
Model 2							
Age (years)	-0.206	0.864	-0.039	0.881	-0.047	0.887	0.070
Body mass index (kg/m^2)	-0.828	-0.057	-0.700	-0.442	-0.744	-0.278	0.292
Gender	-	-	-	-	0.061	0.076	0.959
Skeletal muscle GU	0.837	-0.051	0.844	0.162	0.848	0.039	0.047
Subcutaneous adipose tissue GU	0.458	0.662	0.846	-0.130	0.724	0.065	0.233
Liver GU	0.513	0.423	0.193	0.768	0.322	0.684	0.011
Variance explained (%)	38	27	39	32	32	22	18

effect of age on the rates of GU in adipose tissue and liver in men, but only on liver GU in women. In PCA analysis including both genders, the three PCs explained 72% of the variation. We performed similar PCA using intraperitoneal adipose tissue GU instead of abdominal subcutaneous adipose tissue GU and received largely similar results (Supplementary Table 1, see section on supplementary data given at the end of this article).

We also performed PCA analysis where liver GU was replaced by EGP (Table 3). Skeletal muscle and adipose tissue GUs had positive loadings on PC1 in both genders, whereas EGP showed negative loading in women, and the lack of association in men (Table 3). In women, age and EGP loaded positively and BMI inversely on PC2. Men showed a similar pattern except for BMI, which had a weak association with EGP. Age had a positive loading with subcutaneous fat GU and EGP. When intraperitoneal adipose tissue GU was used in PCA, men had similar results when compared to the analysis using subcutaneous adipose tissue GU, but in women,

intraperitoneal adipose tissue GU was not associated with EGP (Supplementary Table 2).

Discussion

The associations of insulin sensitivity measured by the rates of GU into skeletal muscle, adipose tissue, and liver using the PET technique has not been previously investigated in a single study including a large number of participants. First, we showed that the rates of GU in skeletal muscle and adipose tissue were strongly correlated with each other and with the rates of whole body GU. By contrast, the correlation of liver GU with whole body GU was substantially weaker, and the correlation with skeletal muscle GU was not statistically significant. Secondly, EGP inversely correlated with whole body and skeletal muscle GU in both genders, and with subcutaneous adipose tissue and liver GU in women, but in men, EGP positively correlated with

Table 3 Principal component analysis. Loadings in men and women indicate the contribution of each variable (GU, glucose uptake) to principal components (PC1, PC2, PC3). Liver GU was replaced by endogenous glucose production (EGP).

GU/EGP ($\mu\text{mol/kg tissue/min}$)	Men		Women		All		
	PC1	PC2	PC1	PC2	PC1	PC2	PC3
Model 1							
Age (years)	-0.206	0.741	0.079	0.909	0.241	-0.131	0.884
Body mass index (kg/m^2)	-0.901	-0.117	-0.541	-0.774	-0.855	0.157	-0.232
Gender	-	-	-	-	-0.156	0.667	0.602
Skeletal muscle GU	0.816	-0.314	0.783	0.294	0.804	0.341	-0.127
Subcutaneous adipose tissue GU	0.562	0.644	0.765	0.147	0.703	-0.079	0.119
EGP	0.024	0.719	-0.684	0.547	-0.056	-0.886	0.159
Variance explained (%)	37	32	39	37	33	23	21

adipose tissue GU, but not with liver GU. Thirdly, PCA analysis (Table 2) demonstrated that the rates of GU in skeletal muscle, adipose tissue and liver had high loadings on PC1, and that obesity was negatively associated with the rates of GU similarly in all insulin-sensitive tissues in both men and women. Age was positively associated with GU in adipose tissue and in liver in men, but only with GU in liver in women (PC2). Furthermore, we provided information about distribution of tissue GUs and EGP during insulin stimulation among insulin-resistant and -sensitive subjects and cutoff values, which may be useful for determining what values can be considered normal.

Skeletal muscle takes the major part of GU during insulin stimulation in healthy individuals. We used quadriceps femoris to represent skeletal muscle in our study because its large size, very high correlation with whole body GU (Fig. 1) and important role in daily activities. Proportion of GU into adipose tissue and liver is substantially smaller than in skeletal muscle (1). Given the similarities of insulin signaling in skeletal muscle and adipose tissue, it was not surprising that there was a strong correlation of the rates of GU in these tissues (39). Insulin also suppresses lipolysis in adipose tissue by decreasing FFA concentration in the circulating blood. Impaired insulin's antilipolytic effect in adipose tissue leads to a high flux of FFAs into the liver, and consequently to an increase in triglyceride synthesis. Additionally, high levels of FFAs impair GU in skeletal muscle and adipose tissue (40, 41). In line with previous studies, FFA concentration during the euglycemic clamp in our study negatively correlated with the rates of GU in skeletal muscle, adipose tissue and liver.

In the postprandial state about one-third of ingested glucose is taken up by the liver and stored as glycogen in individuals with normal glucose tolerance (12). Elevated insulin levels stimulate insulin signaling in the liver that promotes glycogen synthesis and lipogenesis and suppresses glycogen breakdown (42). Hepatic gluconeogenesis from non-glucose precursors (lactate, pyruvate, glycerol and amino acids) and glycogen breakdown (glycogenolysis) are the two processes responsible for EGP (43). We found that there was no difference between men and women in liver GU, but men had higher EGP than women, which agrees with a previous study (19). Moreover, men had worse insulin-mediated suppression of lipolysis, which may contribute to the higher EGP (42). EGP correlated inversely and significantly with whole body GU and skeletal muscle GU in women, but only nominally in men.

By applying PC analysis, we wanted to determine if GU in major insulin-sensitive tissues is similarly changed during the euglycemic clamp. Skeletal muscle and adipose tissue GU had high loadings on PC1 but adding liver GU in Model 2 reduced total variation explained by this component (from 45 to 38% in men, from 49 to 39% in women). This suggests that the regulation of GU in the liver differs from that of skeletal muscle and adipose tissue GU without any major differences between men and women. When liver GU was replaced by EGP (another measure of liver insulin resistance) in PC analysis, EGP loaded weakly on PC1, whereas in women, EGP had a negative loading. In women, the effect of age and BMI on EGP was more pronounced than in men.

ROC analysis allowed us to calculate cutoff values which can be used to assess whether a person is insulin sensitive or resistant according to skeletal muscle ($33 \mu\text{mol/kg tissue/min}$) or subcutaneous adipose tissue GU ($11.5 \mu\text{mol/kg tissue/min}$) or EGP ($3 \mu\text{mol/kg body weight/min}$) during euglycemic-hyperinsulinemic clamp using insulin infusion rate of $40 \text{ mU/body surface area m}^2/\text{min}$. Separation of the insulin-sensitive and -resistant groups was clear with the cutoff for skeletal muscle GU in the whole group and subcutaneous adipose tissue and EGP in women. Even though area under ROC curve was lower than 0.7 when calculating thresholds for subcutaneous adipose tissue and EGP measurements in men, the found cutoffs were similar as for women. Thus, these cutoffs may be useful when interpreting quantitative values of tissue GU or EGP in future studies.

This study has some limitations. After a meal, glucose gradient between portal vein and liver cells has major impact on liver glucose uptake; however, we could not measure this effect due to lack of reliable model for $^{18}\text{F-FDG}$ and glucose kinetics in the non-steady glycemic state after meal. Nevertheless, by using euglycemic hyperinsulinemia, we were able to study insulin sensitivity of liver GU, which contributes to glucose clearance after a meal. In addition, it would have been more elegant to compare GU and EGP between fasting state and hyperinsulinemia to measure insulin sensitivity. However, because this study was conducted by combining previously performed research, where several substudies were interventions, radiation exposure and time and resource constraints limited the possibility to include fasting GU measurement to the protocols. Still, since insulin-stimulated GU can be several times higher compared to GU at fasting state in skeletal muscle and adipose tissue and 2-fold higher in the liver, and EGP may be completely suppressed, major

part of the variation in these measures in this study can be explained by insulin sensitivity.

In conclusion, we have provided threshold values, which can be used to identify tissue-specific insulin resistance. Our results suggest that insulin resistance measured by GU is partially similar in all insulin-sensitive tissues, skeletal muscle, adipose tissue and liver and are affected by obesity, aging and gender. Liver GU and EGP did not explain the variance beyond that contributed by skeletal muscle and adipose tissue GU, suggesting that the mechanisms responsible for liver insulin resistance differ from those present in skeletal muscle and adipose tissue. A crosstalk between insulin-sensitive tissues, especially insulin's antilipolytic effects in adipose tissue affecting skeletal muscle GU, and liver function and EGP, are at least in part explaining the differences between the insulin-sensitive tissues.

Supplementary data

This is linked to the online version of the paper at <https://doi.org/10.1530/EJE-17-0882>.

Declaration of interest

The authors declare that there is no conflict of interest that could be perceived as prejudicing the impartiality of this study.

Funding

The study has been conducted at the Center of Excellence in Cardiovascular and Metabolic Diseases, supported by the Academy of Finland, the University of Turku, Turku University Hospital and Åbo Akademi University. It was supported also by the Finnish Cultural Foundation, Varsinais-Suomi Regional fund, Yrjö Jahnsso Foundation, Turku University Foundation, University of Turku, Combined Research Fund and Oskar Öflund Stiftelse.

Author contribution statement

M J H contributed to conception of the work, analysis of the data, interpretation of the results and writing the manuscript. A L R, M B, K A V, J C H and K K K acquired data and revised the manuscript. P N contributed to conception of the work, interpretation of the results, revised the manuscript and supervised the work. All authors accepted the manuscript to be published.

References

- DeFronzo RA. From the triumvirate to the ominous octet: a new paradigm for the treatment of type 2 diabetes mellitus. *Diabetes* 2009 **58** 773–795. (<https://doi.org/10.2337/db09-9028>)
- Iozzo P, Geisler F, Oikonen V, Mäki M, Takala T, Solin O, Ferrannini E, Knuuti J & Nuutila P. Insulin stimulates liver glucose uptake in humans: an 18F-FDG PET Study. *Journal of Nuclear Medicine* 2003 **44** 682–689.
- Virtanen KA, Lönnroth P, Parkkola R, Peltoniemi P, Asola M, Viljanen T, Tolvanen T, Knuuti J, Rönnemaa T, Huupponen R *et al.* Glucose uptake and perfusion in subcutaneous and visceral adipose tissue during insulin stimulation in nonobese and obese humans. *Journal of Clinical Endocrinology and Metabolism* 2002 **87** 3902–3910. (<https://doi.org/10.1210/jcem.87.8.8761>)
- Utriainen T, Takala T, Luotolahti M, Rönnemaa T, Laine H, Ruotsalainen U, Haaparanta M, Nuutila P & Yki-Järvinen H. Insulin resistance characterizes glucose uptake in skeletal muscle but not in the heart in NIDDM. *Diabetologia* 1998 **41** 555–559. (<https://doi.org/10.1007/s001250050946>)
- Virtanen KA, Iozzo P, Hällsten K, Huupponen R, Parkkola R, Janatuinen T, Lönnqvist F, Viljanen T, Rönnemaa T, Lönnroth P *et al.* Increased fat mass compensates for insulin resistance in abdominal obesity and type 2 diabetes: a positron-emitting tomography study. *Diabetes* 2005 **54** 2720–2726. (<https://doi.org/10.2337/diabetes.54.9.2720>)
- Iozzo P, Hällsten K, Oikonen V, Virtanen KA, Kemppainen J, Solin O, Ferrannini E, Knuuti J & Nuutila P. Insulin-mediated hepatic glucose uptake is impaired in type 2 diabetes: evidence for a relationship with glycemic control. *Journal of Clinical Endocrinology and Metabolism* 2003 **88** 2055–2060. (<https://doi.org/10.1210/jc.2002-021446>)
- Schinner S, Scherbaum WA, Bornstein SR & Barthel A. Molecular mechanisms of insulin resistance. *Diabetic Medicine* 2005 **22** 674–682. (<https://doi.org/10.1111/j.1464-5491.2005.01566.x>)
- Molina SA, Moriarty HK, Infield DT, Imhoff BR, Vance RJ, Kim AH, Hansen JM, Hunt WR, Koval M & McCarty NA. Insulin signaling via the PI3-kinase/Akt pathway regulates airway glucose uptake and barrier function in a CFTR-dependent manner. *American Journal of Physiology: Lung Cellular and Molecular Physiology* 2017 **312** L688–L702. (<https://doi.org/10.1152/ajplung.00364.2016>)
- Li X, Monks B, Ge Q & Birnbaum MJ. Akt/PKB regulates hepatic metabolism by directly inhibiting PGC-1 α transcription coactivator. *Nature* 2007 **447** 1012–1016. (<https://doi.org/10.1038/nature05861>)
- Wan M, Leavens KF, Hunter RW, Koren S, von Wilamowitz-Moellendorff A, Lu M, Satapati S, Chu Q, Sakamoto K, Burgess SC *et al.* A noncanonical, GSK3-independent pathway controls postprandial hepatic glycogen deposition. *Cell Metabolism* 2013 **18** 99–105. (<https://doi.org/10.1016/j.cmet.2013.06.001>)
- Perry RJ, Camporez JP, Kursawe R, Titchenell PM, Zhang D, Perry CJ, Jurczak MJ, Abudukadier A, Han MS, Zhang XM *et al.* Hepatic acetyl CoA links adipose tissue inflammation to hepatic insulin resistance and type 2 diabetes. *Cell* 2015 **160** 745–758. (<https://doi.org/10.1016/j.cell.2015.01.012>)
- Winnick JJ, An Z, Moore MC, Ramnanan CJ, Farmer B, Shiota M & Cherrington AD. A physiological increase in the hepatic glycogen level does not affect the response of net hepatic glucose uptake to insulin. *American Journal of Physiology: Endocrinology and Metabolism* 2009 **297** E358–E366. (<https://doi.org/10.1152/ajpendo.00043.2009>)
- Lackey DE & Olefsky JM. Regulation of metabolism by the innate immune system. *Nature Reviews Endocrinology* 2016 **12** 15–28. (<https://doi.org/10.1038/nrendo.2015.189>)
- Samuel VT & Shulman GI. The pathogenesis of insulin resistance: integrating signaling pathways and substrate flux. *Journal of Clinical Investigation* 2016 **126** 12–22. (<https://doi.org/10.1172/JCI77812>)
- Choi KM. The impact of organokines on insulin resistance, inflammation, and atherosclerosis. *Endocrinology and Metabolism* 2016 **31** 1–6. (<https://doi.org/10.3803/EnM.2016.31.1.1>)
- Conte C, Fabbrini E, Kars M, Mittendorfer B, Patterson BW & Klein S. Multiorgan insulin sensitivity in lean and obese subjects. *Diabetes Care* 2012 **35** 1316–1321. (<https://doi.org/10.2337/dc11-1951>)
- Lomonaco R, Ortiz-Lopez C, Orsak B, Webb A, Hardies J, Darland C, Finch J, Gastaldelli A, Harrison S, Tio F *et al.* Effect of adipose tissue insulin resistance on metabolic parameters and liver histology in

- obese patients with nonalcoholic fatty liver disease. *Hepatology* 2012 **55** 1389–1397. (<https://doi.org/10.1002/hep.25539>)
- 18 Korenblat KM, Fabbri E, Mohammed BS & Klein S. Liver, muscle, and adipose tissue insulin action is directly related to intrahepatic triglyceride content in obese subjects. *Gastroenterology* 2008 **134** 1369–1375. (<https://doi.org/10.1053/j.gastro.2008.01.075>)
- 19 Ter Horst KW, Gilijamse PW, de Weijer BA, Kilicarslan M, Ackermans MT, Nederveen AJ, Nieuwdorp M, Romijn JA & Serlie MJ. Sexual dimorphism in hepatic, adipose tissue, and peripheral tissue insulin sensitivity in obese humans. *Frontiers in Endocrinology* 2015 **6** 182. (<https://doi.org/10.3389/fendo.2015.00182>)
- 20 Ter Horst KW, Gilijamse PW, Ackermans MT, Soeters MR, Nieuwdorp M, Romijn JA & Serlie MJ. Impaired insulin action in the liver, but not in adipose tissue or muscle, is a distinct metabolic feature of impaired fasting glucose in obese humans. *Metabolism: Clinical and Experimental* 2016 **65** 757–763. (<https://doi.org/10.1016/j.metabol.2016.02.010>)
- 21 DeFronzo RA, Tobin JD & Andres R. Glucose clamp technique: a method for quantifying insulin secretion and resistance. *American Journal of Physiology* 1979 **237** E214–E223. (<https://doi.org/10.1152/ajpendo.1979.237.3.E214>)
- 22 Dadson P, Landini L, Helmio M, Hannukainen JC, Immonen H, Honka MJ, Bucci M, Savisto N, Soinio M, Salminen P *et al.* Effect of bariatric surgery on adipose tissue glucose metabolism in different depots in patients with or without type 2 diabetes. *Diabetes Care* 2016 **39** 292–299. (<https://doi.org/10.2337/dc15-1447>)
- 23 Mitrou P, Boutati E, Lambadiari V, Maratou E, Papakonstantinou A, Komesidou V, Sidossis L, Tountas N, Katsilambros N, Economopoulos T *et al.* Rates of glucose uptake in adipose tissue and muscle in vivo after a mixed meal in women with morbid obesity. *Journal of Clinical Endocrinology and Metabolism* 2009 **94** 2958–2961. (<https://doi.org/10.1210/jc.2008-2297>)
- 24 American Diabetes Association. Diagnosis and classification of diabetes mellitus. *Diabetes Care* 2006 **29** (Supplement 1) S43–S48.
- 25 Peltoniemi P, Lönnroth P, Laine H, Oikonen V, Tolvanen T, Grönroos T, Strindberg L, Knuuti J & Nuutila P. Lumped constant for [(18)F]fluorodeoxyglucose in skeletal muscles of obese and nonobese humans. *American Journal of Physiology: Endocrinology and Metabolism* 2000 **279** E1122–E1130. (<https://doi.org/10.1152/ajpendo.2000.279.5.E1122>)
- 26 Virtanen KA, Peltoniemi P, Marjamäki P, Asola M, Strindberg L, Parkkola R, Huupponen R, Knuuti J, Lönnroth P & Nuutila P. Human adipose tissue glucose uptake determined using [(18)F]-fluoro-deoxy-glucose ([18F]FDG) and PET in combination with microdialysis. *Diabetologia* 2001 **44** 2171–2179. (<https://doi.org/10.1007/s001250100026>)
- 27 Hamacher K, Coenen HH & Stocklin G. Efficient stereospecific synthesis of no-carrier-added 2-[18F]-fluoro-2-deoxy-D-glucose using aminopolyether supported nucleophilic substitution. *Journal of Nuclear Medicine* 1986 **27** 235–238.
- 28 Alenius S & Ruotsalainen U. Bayesian image reconstruction for emission tomography based on median root prior. *European Journal of Nuclear Medicine* 1997 **24** 258–265.
- 29 Patlak CS & Blasberg RG. Graphical evaluation of blood-to-brain transfer constants from multiple-time uptake data. Generalizations. *Journal of Cerebral Blood Flow and Metabolism* 1985 **5** 584–590. (<https://doi.org/10.1038/jcbfm.1985.87>)
- 30 Gjedde A. Calculation of cerebral glucose phosphorylation from brain uptake of glucose analogs in vivo: a re-examination. *Brain Research* 1982 **257** 237–274. ([https://doi.org/10.1016/0165-0173\(82\)90018-2](https://doi.org/10.1016/0165-0173(82)90018-2))
- 31 Iozzo P, Jarvisalo MJ, Kiss J, Borra R, Naum GA, Viljanen A, Viljanen T, Gastaldelli A, Buzzigoli E, Guiducci L *et al.* Quantification of liver glucose metabolism by positron emission tomography: validation study in pigs. *Gastroenterology* 2007 **132** 531–542. (<https://doi.org/10.1053/j.gastro.2006.12.040>)
- 32 Iozzo P, Gastaldelli A, Jarvisalo MJ, Kiss J, Borra R, Buzzigoli E, Viljanen A, Naum G, Viljanen T, Oikonen V *et al.* 18F-FDG assessment of glucose disposal and production rates during fasting and insulin stimulation: a validation study. *Journal of Nuclear Medicine* 2006 **47** 1016–1022.
- 33 Wickham H. *Ggplot2: Elegant Graphics for Data Analysis*, pp 1–213. New York: Springer-Verlag, 2009. (<https://doi.org/10.1007/978-0-387-98141-3>)
- 34 R Core Team. *R: A Language and Environment for Statistical Computing*. Vienna, Austria: R Foundation for Statistical Computing, 2017. (<https://doi.org/10.1007/b98835>)
- 35 Jolliffe IT. *Principal Component Analysis*, p 488. New York: Springer-Verlag, 2002. (<https://doi.org/10.1007/b98835>)
- 36 Kaiser HF. The application of electronic computers to factor analysis. *Educational and Psychological Measurement* 1960 **20** 141–151. (<https://doi.org/10.1177/001316446002000116>)
- 37 Stern SE, Williams K, Ferrannini E, DeFronzo RA, Bogardus C & Stern MP. Identification of individuals with insulin resistance using routine clinical measurements. *Diabetes* 2005 **54** 333–339. (<https://doi.org/10.2337/diabetes.54.2.333>)
- 38 Hosmer DW & Lemeshow S. Assessing the fit of the model. In *Applied Logistic Regression*, ch. 5, pp 143–202. New York, USA: John Wiley & Sons, Inc., 2000. (<https://doi.org/10.1002/0471722146>)
- 39 Rask-Madsen C & Kahn CR. Tissue-specific insulin signaling, metabolic syndrome, and cardiovascular disease. *Arteriosclerosis, Thrombosis, and Vascular Biology* 2012 **32** 2052–2059. (<https://doi.org/10.1161/ATVBAHA.111.241919>)
- 40 Iozzo P, Lautamäki R, Geisler F, Virtanen KA, Oikonen V, Haaparanta M, Yki-Järvinen H, Ferrannini E, Knuuti J & Nuutila P. Non-esterified fatty acids impair insulin-mediated glucose uptake and disposition in the liver. *Diabetologia* 2004 **47** 1149–1156. (<https://doi.org/10.1007/s00125-004-1443-2>)
- 41 Nuutila P, Koivisto VA, Knuuti J, Ruotsalainen U, Teräs M, Haaparanta M, Bergman J, Solin O, Voipio-Pulkki LM & Wegelius U. Glucose-free fatty acid cycle operates in human heart and skeletal muscle in vivo. *Journal of Clinical Investigation* 1992 **89** 1767–1774. (<https://doi.org/10.1172/JCI115780>)
- 42 Sharabi K, Tavares CDJ, Rines AK & Puigserver P. Molecular pathophysiology of hepatic glucose production. *Molecular Aspects of Medicine* 2015 **46** 21–33. (<https://doi.org/10.1016/j.mam.2015.09.003>)
- 43 Wahren J & Ekberg K. Splanchnic regulation of glucose production. *Annual Review of Nutrition* 2007 **27** 329–345. (<https://doi.org/10.1146/annurev.nutr.27.061406.093806>)

Received 24 October 2017

Revised version received 7 March 2018

Accepted 12 March 2018